Electrowetting of Complex Fluids: Perspectives for Rheometry on Chip

A. G. Banpurkar,† M. H. G. Duits,* D. van den Ende, and F. Mugele

Physics of Complex Fluids, Faculty of Science and Technology, IMPACT and MESA+ Institutes, University of Twente, P.O. Box 217, 7500AE Enschede, The Netherlands

Received September 19, 2008. Revised Manuscript Received November 5, 2008

We explore the possibilities of electrowetting (EW) as a tool to assess the elastic properties of aqueous jellifying materials present in the form of a small droplet on a hydrophobic substrate. We monitored the EW response of aqueous solutions of gelatin (2−10 wt %) in ambient oil for various temperatures (8−40 °C) below and above the gel point. Whereas the drops remained approximately spherical cap-shaped under all conditions, the voltage-induced reduction of the contact angle became progressively less pronounced upon entering the gel state at lower temperatures. We modeled the decrease in contact angle by minimizing the total energy of the drops consisting of interfacial energies, electrostatic energy, and the elastic energy due to the deformation of the drop, which was taken into account in a modified Hertz model. This allowed fitting the data and extracting the elastic modulus G, which were found to agree well with macroscopic storage moduli G' obtained with oscillatory shear rheometry. These results show that EW can be used as a tool for characterizing soft materials with the elastic moduli ranging (at least) from 10 to 1000 Pa. Our observations also create interesting perspectives for performing in situ rheological measurement inside microfluidic chips.

1. Introduction

In the past five years, a growing number of papers have reported on the formation, transport, mixing, and (biological, chemical) analysis of droplets in microfluidic chips.[1−8] One reason for the interest in this particular variant of Laboratory-on-a-Chip is that droplets provide a constrained environment, in which the concentrations of the droplet constituents can be precisely defined. This allows us to control or measure analyte concentrations or to assume mass conservation (in the case of chemical reactions). The only fundamental requirements are that the droplet-surrounding medium (usually oil) is immiscible with the (usually aqueous) droplet phase and impermeable to the molecules solved in the latter.

A special class within this droplet-based technology is that of so-called digital microfluidics,[4−8] in which the droplets are handled in discrete time- or displacement steps. In this application, droplets can be manipulated to make discrete steps, to be mixed for a certain amount of time, or kept at a detection site for a given duration. It is even possible to keep track of the history and location of each individual droplet. The most frequent application of digital microfluidics is found in electrowetting (EW).[8−10] Here, the digital character is obtained by patterning discrete and individually addressable microelectrodes onto a nonconducting substrate like glass or a plastic. In the presence of a hydrophobic surface coating, aqueous droplets can then be drawn toward the electrodes of interest by electrically activating them. This is the basic step via which droplet transport, mixing, coalescence, and splitting are all realized.

But, in fact, EW is even more versatile because it is not limited to digital operations only. Having well-defined control surfaces, the functional dependence of the droplet's local contact angle on the applied electrode voltage (i.e., the principle underlying the digital control) can be quantitatively described with the electrowetting equation, often formulated as a linear relation between $\cos\theta$ and U^2, with θ the contact angle and U the applied voltage. This equation, derived from thermodynamics,[9] describes how the equilibrium contact angle is set by the competition between electric stress and interfacial tension. Interference with this balance (e.g. by changing the interfacial tension) will then lead to changes in the contact angle, which can be precisely measured.

Considering these possibilities, it is rather remarkable that the EW principle has hardly been utilized (for notable exceptions see ref 10) for handling and analyzing aqueous fluids containing supramolecular compounds like polymers or colloids. Such fluids, generally having a composition-dependent interfacial tension and a more complex (i.e., non-Newtonian) rheology, are potentially very well suited for manipulations *and* characterization with EW. In a recent study,[11] we demonstrated that EW can be used to quantitatively measure interfacial tensions of a variety of surfactant and biopolymer solutions.

In the present communication, we extend the applicability of the EW as a quantitative tool for soft-matter materials characterization to rheological properties of the drop phase. For non-Newtonian fluids, there are additional contributions to the force balance. These can be viscous as well as elastic forces, depending on the nature of the deformation (i.e., static or dynamic) and the rheological signature of the droplet phase (i.e., viscous, viscoelastic, elastic). These additional contributions modify the (transient or steady) shape response of the droplet, which can then be measured optically or electrically. Given this potential, it will be very interesting to explore the possibility of using EW for rheometry. The results can then be compared with existing

* To whom correspondence should be addressed. E-mail: M.H.G.Duits@utwente.nl.

† Also at the Center for Advanced Studies in Materials Science and Condensed Matter Physics, Department of Physics, University of Pune, Pune 411 007, India

(1) Teh, S. Y.; Lin, R.; Hung, L. H.; Lee, A. P. *Lab Chip* **2008**, *8*(2), 198–220.
(2) Haeberle, S.; Zengerle, R. *Lab Chip* **2007**, *7*(9), 1094–1110.
(3) Song, H.; Chen, D. L.; Ismagilov, R. F. *Angew. Chem.,Int. Ed.* **2006**, *45*(44), 7336–7356.
(4) Fair, R. B. *Microfluidics Nanofluidics* **2007**, *3*(3), 245–281.
(5) Piggee, C. *Anal. Chem.* **2007**, *79*(23), 8828–8828.
(6) Cheow, L. F.; Yobas, L.; Kwong, D. L. *Appl. Phys. Lett.* 2007; *90*, 5, Art. No. 054107.
(7) Griffith, E. J.; Akella, S. *Int. J. Robotics Research* **2005**, *24*(11), 933–949.
(8) Cho, S. K.; Moon, H. J.; Kim, C. J. *J. Microelectr. Mech. Syst.* **2003**, *12*(1), 70–80.
(9) Mugele, F.; Baret, J.-C. *J. Phys.: Condens. Matter* **2005**, *17*(28), R705–R774.
(10) Srinivasan, V.; Pamula, V. K.; Fair, R. B. *Lab Chip* **2004**, *4*, 310.
(11) Banpurkar, A. G.; Nichols, K. P.; Mugele, F. *Langmuir* **2008**, *24*(19), 10549–10551.

10.1021/la803080k CCC: $40.75
Published on Web 12/11/2008

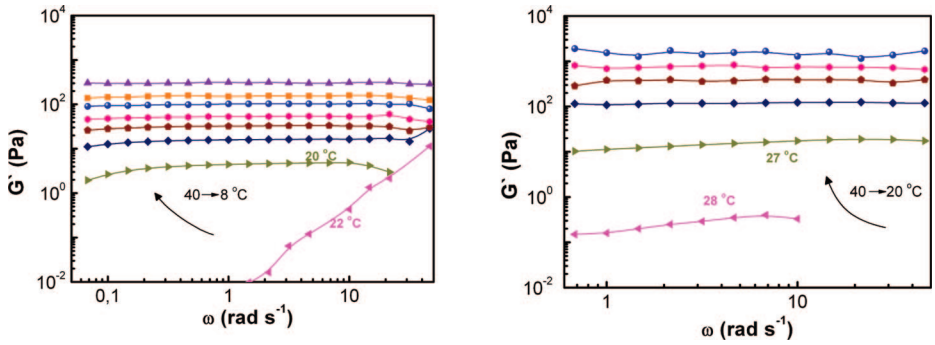

Figure 1. Frequency dependence of the storage modulus for 2 and 10 wt % gelatin solutions (left respectively right). For clarity, some temperatures have been left out. The chronological order is indicated by the arrows; left panel: 22, 20, 19, 18, 17, 15, 13, and 8 °C; right panel: 28, 27, 26, 25, 24, and 20 °C.

droplet-based methods like the microfluidic comparator,[12−14] measurements of drop deformation in constriction and expansion flows,[15,16] or AFM in force−distance mode,[17−19] where it is far from trivial to extract quantitative rheological measures.

In this article, we explore these possibilities through EW experiments on aqueous gelatin droplets, in both liquid and solid states. Using the generic substrate/wire geometry, we measured the voltage dependence of the contact angle for millimeter-sized droplets, resting on Teflon-coated surfaces and immersed in an oil phase. The tunability of the gelatin's stiffness via the temperature is used to study the relation between electric field, droplet deformation, and elastic modulus. To extract quantitative moduli from the experimental data, we developed a model in which the contribution of elasticity to the total energy is described with a modification of the Hertz model,[20] suitable for small deformations. The Young's modulus E and hence also the shear modulus G can then be obtained by fitting $\Delta \cos \theta$ versus U^2. Subsequently, these G data are compared to classical rheological measurements of the storage modulus $G'(\omega)$ in the low-frequency limit ($\omega \rightarrow 0$). By doing so for several concentrations and temperatures, we examine the correspondence with macrorheology and establish the range of elastic moduli that can be measured with EW.

2. Materials and Methods

2.1. Preparation of Gelatin Solutions and Gels. Gelatin powder (from an alkali-treated source, isoelectric point at pH 5, and Bloom strength 180 g) was kindly provided by Delft Gelatin BV, The Netherlands. Gelatin solutions were prepared as follows: A known amount (2, 5, or 10 wt %) of gelatin powder was left to soak in deionized (DI) water at 50 °C for 20 min, whereafter a small amount of 0.1 mM NaCl solution was added to increase the conductivity to 2.5 mS/cm. Maintaining temperature at 50 °C, the gelatin solution was homogenized for 1 h using a magnetic stirrer, after which bubbles were removed by sonication for 20 min. This clear solution was then packed in screwcap bottles and stored overnight in a refrigerator at 4 °C. We found that all solutions transformed to a gel state. Prior to experiments, samples were heated in a water bath at 50 °C for 30 min to restore the liquid state, after which the gelatin solution was either injected as a droplet into the oil phase (EW) or pipetted onto the plate of the measuring geometry (rheology). Both of these environments were at 40 °C during injection.

For the oils, we used analytical grade silicone oil (AK5, Fluka) with $\gamma = 19.2$ mNm^{-1} and n-dodecane (99+ % purity, Aldrich) with $\gamma = 25.4$ mNm^{-1} (measured against water). In a side experiment, Span 80 surfactant (sorbitan monooleate, Fluka) with an hydrophilic lipophilic balance value of 4.3 was solved up to 0.1 wt % (2.33 mM, i.e., $\gg$0.3 mM, the cmc) into dodecane and homogenized by stirring for 1 h. This was done to minimize the O/W interfacial tension while also ensuring a fast equilibration.

2.2. Macroscopic Rheology. Oscillatory shear measurements were performed using a Haake RS600 controlled stress rheometer, equipped with a vapor lock (filled with mineral oil) to prevent water evaporation. Measurements at 2, 5, and 10 wt % gelatin were done using a cone-plate geometry (diameter 60 mm, cone angle 2°). In each experiment, 2.0 mL of gelatin solution was introduced with both the fluid and the measuring geometry preheated at 40 °C. Because it takes time for a gel to form, as well as to adapt to a new temperature once formed, we standardized our time−temperature protocol in both macrorheology and EW experiments. Temperature was lowered stepwise, with the stepsize being at least 1 °C, the average rate varying between 2.5 and 4 °C/hr, and a minimum waiting time of 15 min per temperature. Oscillatory shear force measurements were carried out between 0.01 and 50 Hz at a stress amplitude of 0.02 Pa. For gels with a storage modulus >1 Pa (as in our case), this corresponds to a strain <2%, which is well within the linear regime of gelatin.[21]

Figure 1 shows the storage moduli $G'(\omega)$ measured for the 2 and 10 wt % gelatin solutions. On decreasing temperature, a sharp transition occurs after which $G'(\omega)$ becomes measurable as a frequency-independent function. The gelation temperatures corresponding to 2, 5, and 10 wt % were found at 20, 26, and 27 °C, respectively. In the gel regimes, the loss moduli $G''(\omega)$ (data not shown) were always $<0.1*G'(\omega)$ as often found for gels. These characteristics for $G'(\omega)$ and $G''(\omega)$ seem to justify the interpretation of the plateau value of $G'(\omega)$ as an equilibrium storage modulus G_0,[22] as will be used in the comparison with EW microrheology.

2.3. Surface Tension Measurements. The interfacial tensions of a 2 wt % gelatin solution with respect to three surrounding oils (silicone, dodecane, and dodecane + Span 80) were measured at 30 °C using a commercial tensiometer (*K*-11, Krüss, Germany) operated in the standard DuNoüy ring mode. The data were averaged over 20 individual sets. In respective order, the following values were found: 20.2, 11.6, and 6.6 mN/m. In the analysis to be described in section 3.3, we have assumed that the changes in surface tension on lowering temperature to around 10 °C are negligible. Prior to the

(12) Abkarian, M.; Faivre, M.; Stone, H. A. *Proc. Natl. Acad. Sci. U.S.A.* **2005**, *103*, 538–542.
(13) Vanapalli, S. A.; van den Ende, D.; Duits, M. H. G.; Mugele, F. *Appl. Phys. Lett.* **2007**, *90*, 114109.
(14) Vanapalli, S. A.; Banpurkar, A. G.; van den Ende, D.; Duits, M. H. G.; Mugele, F. *Lab-on-a-Chip*, in press.
(15) Hudson, S. D.; Cabral, J. T.; Goodrum, W. J.; Beers, K. L.; Amis, E. J. *Appl. Phys. Lett.* **2005**, *87*, 081905.
(16) Taylor, G. I. *Proc. R. Soc. London* **1934**, 146–501.
(17) Filip, D.; Uricanu, V. I.; Duits, M. H. G.; Agterof, W. G. M.; Mellema, J. *Langmuir* **2005**, *21*, 115.
(18) Attard, P.; Miklavcic, S. J. *Langmuir* **2001**, *17*(26), 8217–8223. Effective spring constant of bubbles and droplets.
(19) Gillies, G.; Prestidge, C. A. *Adv. Colloid Interface Sci.* **2004**, *108−09*, 197–205.
(20) (H) Hertz, J. *Reine Angew. Math* **1882**, *92*, 156.
(21) Bot, A.; van Amerongen, I. A.; Groot, R. D.; Hoekstra, N. L.; Agterof, W. G. M. *Pol. Gels Netw.* **1996**, *4*(3), 189–227.
(22) 1 Derooij, R.; van den Ende, D.; Duits, M. H. G.; Mellema, J. *Phys. Rev. E* **1994**, *49*(4), 3038–3049.

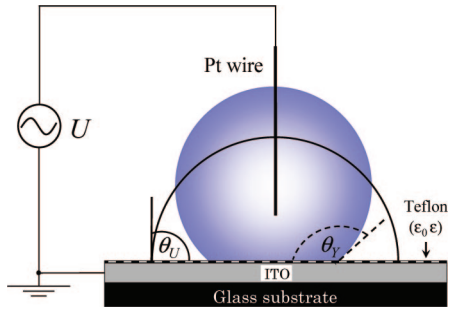

Figure 2. Setup used to study electrowetting of gelatin/water droplets. The platinum wire together with the ITO layer covered by a Teflon layer form an electrical circuit in which the droplet serves as a one of the capacitor plates with adjustable surface area. By applying an ac voltage, a decrease in the contact angle (and hence an increase in area, capacitance) can be induced without causing polarization at the electrodes. Changing the (rms) voltage from 0 to U causes a change from the Young's contact angle θ_Y (dashed) to θ_U (solid).

measurements, a standard water/silicone oil sample had been measured for instrument calibration.

2.4. Preparation of EW Substrates. To obtain the dielectric substrate, a glass slide with a precoated (conductive) Indium Tin Oxide (ITO) layer was covered with a uniform layer of Teflon AF (1600) following the recipe described in ref 23. Briefly, the ITO-glass was dipcoated in a 6 vol % solution of amorphous Teflon AF (1600) fluoropolymer in perfluorinated solvent (FC 75), and subsequently retracted at 15 cm/min. Then, the film was kept in an oven at 110 °C for 10 min. After repeating this coating and drying step once, the substrate was treated at 160 °C for 10 min and 340 °C for 30 min in vacuum (~100 mTorr) for complete removal of the solvent. The average thickness of the resulting Teflon layer was measured by both AFM and EW,[11] yielding $d = 4.4 \pm 0.2$ and 4.4 ± 0.2 μm, respectively. Aqueous solutions were found to partially wet the Teflon surface with equilibrium Young's angles $\theta_Y = \sim 170-160$ ° (in oil) and $120-110$° (in air).

2.5. EW Experiments. For the majority of our experiments, we used a generic EW setup[9] as shown in Figure 2. Droplets of volume $2-20$ μL were deposited onto a planar EW substrate placed at the bottom of a cubic glass cell filled with oil. A platinum wire (radius $r = 25$ μm) cleaned with alcohol and subsequently passed through a flame (to avoid contaminations) was plunged into the drop. The cell was then placed on a goniometer whose temperature was maintained using a circulating water bath (Haake K). The temperature of the oil bath close to the droplet was monitored using a k-type thermocouple. Temperature sweeps were performed with the droplet in continuous contact with the substrate after initial contact at 40 °C (i.e., with the droplet in the liquid state).

For the EW control signal, we applied a voltage amplitude ramp carried by a wave with frequency $f_c = 10$ kHz. The rms amplitude was varied between 0 and 110 V using a triangular waveform at a frequency of 0.005 Hz. These ramps were slow enough to allow measurement in real time of the contact angle $\theta(U)$ as a function of the applied voltage U. For this we used an optical contact angle goniometer (OCA-15+, Data Physics, Germany) with built-in SCA-20 software.

3. Results

3.1. Droplet Deformation. In Figure 3, a representative set of images is shown for the same (5 wt %) gelatin/water droplet subjected to EW numbers (eq 2 below) ranging from 0 to 1.0 in the liquid state at 40 °C (top row) and in the gelled state at 18 °C (bottom row). For both temperatures, a decrease in the contact angle can be observed, but clearly the changes are substantially smaller for the gelled droplet. Qualitatively, this result is expected. It confirms that elastic stresses provide an additional restoring force in the gelled state at 18 °C. It is important to note that all drops investigated approximately retained their spherical cap shape, independent of the voltage and the degree of gelation.

To quantify our observations, we extracted the contact angle θ as a function of the voltage U. These measurements are illustrated in Figure 4 for the same droplet as in Figure 3. For the liquid states (i.e., all temperatures above the gel point), all graphs of

$\Delta \cos\theta = \cos\theta(U) - \cos\theta_Y$ vs U^2 were linear, with a slope corresponding quantitatively to the electrowetting equation:[9]

$$\cos\theta(U) = \cos\theta_Y + \frac{\varepsilon\varepsilon_0}{2d\gamma}U^2 \qquad (1)$$

with $\epsilon\epsilon_0$ the dielectric permittivity, θ_Y Young's angle, d the insulator layer thickness, and γ the interfacial tension of the gelatin solution with the oil at 30 °C. The second term in the RHS of eq 1 is also known as the (dimensionless) electrowetting number,

$$\eta = \frac{\varepsilon\varepsilon_0}{2d\gamma}U^2 \qquad (2)$$

which allows comparison between different EW experiments.

Figure 4 shows that $\cos\theta$ remains almost perfectly over the entire range of η even for the gelled droplets ($T < 25$ °C). The change from liquid to solid behavior and the subsequent stiffening of the gel (as temperature is further decreased) only become manifest as a decrease in the slope α of the curve (inset Figure 4). The magnitude of the slope decrease follows an S-shaped curve when plotted as a function of temperature, with the slope itself approaching zero as the gelled droplet becomes stiffer. Then, the stresses induced by the electric field are no longer capable of significantly deforming the droplet.

We note here that the same linear behavior and dependence of the slope on the temperature was also found in a different EW geometry, in which the wire/planar electrode was replaced by a set of two interdigitated electrodes, as in ref 11 (data not shown).

3.2. Repeatability. Macromolecular constituents of complex fluids frequently adsorb to interfaces, which may compromise the reproducibility and the reliability of contact angle measurements. To exclude such detrimental effects, we repeated our EW experiment for almost 1000 times (duration: 20 h). Figure 5 shows the results for a 3 μL drop of 2 wt % gelatin kept at 40 °C. In this particular experiment, the voltage was ramped continuously between 0 and 110 V at 100 s/cycle. By keeping the droplet well above the gel point, we allowed a maximum rate of (normally unwanted) adsorption of the gelatin molecules onto the Teflon substrate and/or the O/W interface. Looking at the data envelope, that is the contact angles at 0 and 110 V, a slight decrease of both angles with time is observed (note the logarithmic time axis). Whereas we cannot exclude that this is due to a slight interfacial adsorption of gelatin molecules, it is clear that the changes in the contact angles are only small, and that the effect on $\Delta\cos\theta$ (which sets the slope in graphs like Figure 4) is even smaller. Considering the electric field of ~25V/μm applied in this experiment, also a slight degradation of the insulator layer (over time) could be responsible for the effect. In any case, it is clear that significant interfacial deposition of gelatin molecules, making the substrate surface hydrophilic or substantially reducing the O/W interfacial tension, does not occur. We speculate that the presence of a (thin) oil layer between the droplet and the substrate[4,24,25] may have contributed to keeping the substrate surface clean.

(23) Seyrat, E.; Hayesa, R. A. *J. Appl. Phys.* **2001**, *90*, 1383.
(24) Quilliet, C.; Berge, B. *Europhys. Lett.* **2002**, *60*(1), 99–105.
(25) Staicu, A.; Mugele, F. *Phys. Rev. Lett.* **2006**, *97*(16), 4.

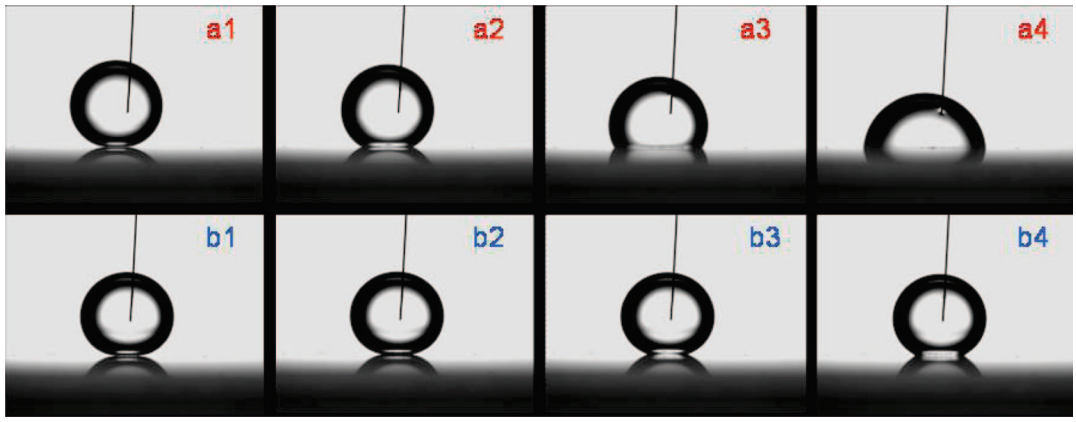

Figure 3. Changes in droplet shape due to electrowetting. At 40 °C (upper panels, a) where the droplet is purely liquid, the same electric field has a much stronger effect on the contact angle than at 18 °C (lower panels, b) where the droplet is gelled. Results are shown for a 5 wt % gelatinized droplet with radius $R_0 = 1.53$ mm. Electrowetting numbers are: 1) 0, 2) 0.11, 3) 0.44, 4) 1.0. This droplet was suspended in silicone oil.

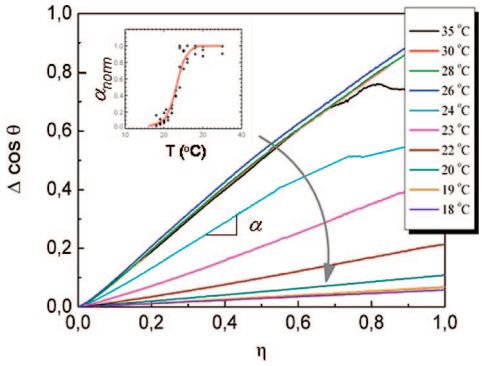

Figure 4. Variation (color online) of the contact angle with the EW voltage, plotted in reduced quantities, for a 15 μL droplet with 5 wt % gelatin in silicone oil at various temperatures (lowered from 35 to 18 °C, following the arrow). Between 35 and 26 °C, all data overlap. Below 25 °C, the slope is reduced, saturating at 18 °C. Inset, slope of EW curves (normalized to that of the liquid state) vs temperature; data from three different drops.

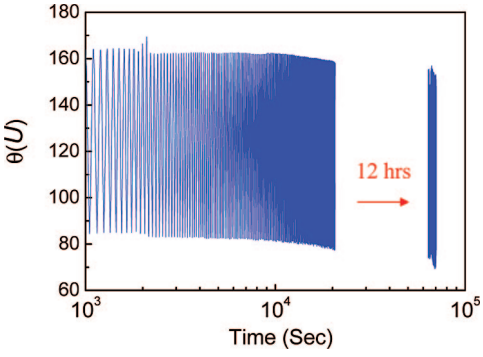

Figure 5. Variation of the contact angle range θ (U) with time in a long-duration EW experiment. A 2 wt % gelatin drop was subjected to repeated (symmetric sawtooth) voltage ramps, where each cycle visited 110 V as the highest voltage, and lasted 100 s. After 5.5 h, the measurements were interrupted for 12 h with the droplet still residing on the substrate.

3.3. Theoretical Modeling. To model the deformation of a gelled droplet in an EW experiment, one has to reconsider the problem of energy minimization for the droplet. Besides the interfacial and electrostatic energy terms, also the energy due to elastic deformation has to be taken into account. Inspired by the fairly spherical shapes observed also for the gelled droplets (especially for $\eta < 0.5$), we simplified the problem by assuming a spherical cap shape (i.e., a constant radius of curvature) for the droplet. Then, the interfacial and electrostatic energies can still be expressed as functions of the (to be optimized) contact angle only. Defining:

$$X = \cos\theta \text{ and } Y = \cos\theta_Y \tag{3}$$

with θ the actual (i.e., voltage dependent) contact angle and θ_Y the Young's angle, the interfacial (W_1) and electrostatic (W_2) energies are then expressed as:

$$W_1 = \gamma\pi R_0^2[2(1-X) - Y(1-X^2)] \text{ and } W_2 = \frac{\pi\varepsilon}{2d}U^2R_0^2 \times (1-X^2) \tag{4}$$

with R the curvature radius of the spherical cap, which is related to the contact angle and the (constant) droplet volume V via:

$$V = \frac{\pi}{3}R^3[2 - 3X + X^3] = \frac{4\pi}{3}R_0^3 \tag{5}$$

Here, R_0 is the radius of the drop in the freely suspended state. To model the elastic deformation energy, we have incorporated the following assumptions: 1) in the (to be considered) regime of small deformations, the elastic modulus can be assumed to remain constant. 2) adhesion between the droplet and the substrate is negligible. For this case, the Hertz model[20] for contact between nonadhesive elastic bodies (with the substrate being much stiffer) should be appropriate.

One aspect that needs special consideration is that, in our case, even in the absence of elastic stress, an apparent deformation exists. This is because in our experimental protocol (section 2.5) the droplets were brought into contact with the substrate at 40 °C (where the gelatin solution is purely liquid) and left there untouched during the subsequent temperature sweep. Because the temperature decrease steps were carried out at zero voltage (grounded electrodes), it can be reasonably assumed that the (stress-free) gel state was reached with the droplet geometry corresponding to the Young's angle. Hence, the starting point of our EW experiments was that of stress-free, slightly flattened drops with apparent indentation:

$$\delta_Y = R(1+Y) \tag{6}$$

Note that because $(1 + Y) \ll 1$, also $R \approx R_0$ as can be seen from eq 5 (substituting X for Y). The elastic energy is described by a modified Hertz formula

$$W_3 = \frac{4}{3}\frac{ER_0^{1/2}}{(1-\nu^2)}\left(\frac{2}{5}\delta^{5/2} - \delta\delta_Y^{3/2}\right) \quad (7)$$

where E is the Young's modulus, ν the Poisson ratio, and δ the actual indentation. Compared to the standard Hertz model (which consists only of the term $\sim\delta^{5/2}$), we subtracted the contribution due to the initial deformation δ_Y in such a way that the elastic forces vanish at zero voltage, that is for $\delta = \delta_Y$. Minimizing the total energy $W = W_1 + W_2 + W_3$ through variation of $X = \cos\theta$ yields:

$$\eta = X - Y + K * H(X, Y) \quad (8)$$

with

$$H(X,Y) = \left(\frac{4^{1/6}(3+X)(1+X)^{3/2}}{(1-X)^{4/3}(2+X)^{1/6}}\right) \times \left(1 - \frac{(1-X)(2+X)^{1/2}(1+Y)^{3/2}}{(1-Y)(2+Y)^{1/2}(1+X)^{3/2}}\right) \quad (9)$$

and

$$K = \frac{2ER_0}{3\gamma\pi(1-\nu^2)} \cong \frac{8GR_0}{3\gamma\pi} \quad (10)$$

where G is the elastic shear modulus. Expressed in the physical quantities of interest, eq 8 can thus be rewritten as:

$$\eta = \cos\theta - \cos\theta_Y + \frac{8GR_0}{3\gamma\pi} * H(\cos\theta, \cos\theta_Y) \quad (11)$$

Note that, in the absence of an elastic modulus, that is for $K = G = 0$, eq 11 reduces to the electrowetting equation (eq 1).

Figure 6 shows the behavior of the contact angle as a function of η, as predicted by the model for increasing values of K. Obviously and most importantly, the model reproduces the decreasing slope of the electrowetting curves, as the experiments found (Figure 4). Moreover, the model curves also display a slight negative curvature, which is absent in the experimental data. Note, however, that this curvature is most pronounced for systems with a small but finite elasticity at large contact-angle variations, that is at large drop deformations. In this regime, the drop deformation is rather strong, and it is hence not surprising to observe deviations from the Hertz model.

Eq 11 also reveals an interesting scaling behavior: because the function $H(\cos\theta, \cos\theta_Y)$ is of order unity over a wide range of values of θ (inset of Figure 6), the elasticity-induced deviation from the ideal EW behavior is determined by a dimensionless ratio GR_0/γ, which measures the relative strength of elastic versus interfacial energies in the system. If this ratio is small compared to unity, surface tension forces determine the drop response, if large elastic forces dominate.

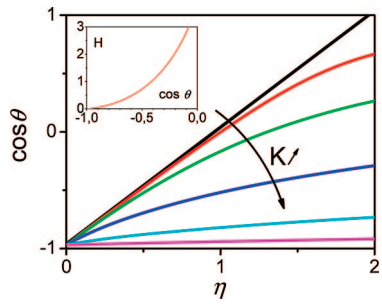

Figure 6. Model prediction (color online) for cos θ vs the electrowetting number for various values of K (0, 0.01, 0.1, 1. 10, 100) for $\theta_Y = 170°$. (For the typical experimental conditions in this work, $G' \approx 15K$ [Pa].) Inset: function $H(\cos\theta, \cos\theta_Y)$ vs cos θ for $\theta_Y = 170°$.

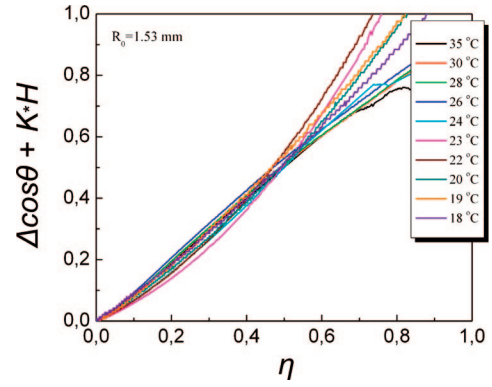

Figure 7. Fitting (color online) of electrowetting data to eq 11. Data set is the same as in Figure 4.

Eq 11 can now be used to fit the experimental data of the contact angle as a function of the voltage, using the previously measured γ, R_0, θ_Y, and d as additional inputs to calculate η from U, where K is the only free parameter. K is obtained by optimizing the correspondence between $K*H(\eta)$ and $\eta - \Delta\cos\theta$. Eq 11 also indicates that the data for different temperatures should collapse onto a single curve by plotting the quantity $\Delta\cos\theta + K*H(\eta)$ versus η. In Figure 7, we show such a plot for the same data as in Figure 4. To avoid the contribution of nonlinear drop deformations, we deduced K by fitting the data only up to an − admittedly somewhat arbitrarily chosen − upper limit $\eta_{max} = 0.5$. Within the fitting range, a fairly good collapse of the data is obtained. Nevertheless, some systematic deviations from the straight master curve are found, which turn out to be the most pronounced at intermediate temperatures. These systematic deviations (which are also responsible for the spreading of the curves for $\eta > \eta_{max}$) are due to the curvature of the model curves discussed above (Figure 6), which remains finite even for low η and which is not present in the experimental data. We have currently no explanation for this deviation.

3.4. Elastic Moduli. Eq 11 suggests that it should be possible to superimpose all experimental data for all droplets (at different size, concentration, and temperature) onto a masterplot of η^* (i.e., RHS(11)) versus η. To assess the validity of our model, we have accordingly plotted data for droplets at 2, 5, and 10 wt % gelatin, for silicone and dodecane oils, for different sized droplets between 3 and 20 μL and for different temperatures in one graph (Figure 8). Again, the fit range for η was limited to 0−0.5 to avoid influences of nonlinearities. For droplets in the pure liquid state, this plot merely provides a check on calibration because the electrowetting equation (eq 1) should be satisfied if the interfacial tension and insulator thickness were measured accurately enough. Gelled drops with significant stiffness present a more specific test of the modified Hertzian approach, and hence these are plotted with different colors and symbols in Figure 8. From this graph, it appears that the generality of the description is quite good, meaning that optimization of the value of K, as needed for extracting the moduli G, is straightforward. The data for the gelled droplets are somewhat curved, which makes the assessment of the optimum value for K slightly dependent on the fit range. To evaluate this effect, we reanalyzed our data with $\eta_{max} = 0.2$. Under these conditions, we found K to increase by typically 10%, with occasional deviations up to 15−20%. Taking these uncertainties as an estimated error in the measurement of G, the accuracy of the EW method is comparable to the typical error in macroscopic rheology.

Finally, we present in Figure 9 the elastic moduli (G) as extracted from the EW data for the three different gelatin

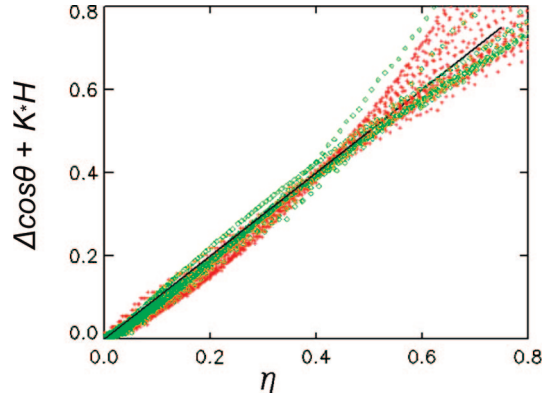

Figure 8. Collapse (color online) of data after normalization of $\eta(X,Y)$ data according to eq 8. Included are data for 2, 5, and 10 wt % gelatin in silicone oil as well as 5 wt % gelatin in dodecane. Green diamonds: droplets in the liquid state. Red crosses: gelled droplets. The solid line indicates the theoretical behavior.

concentrations as a function of temperature. For comparison, also the storage moduli ($G'(\omega \rightarrow 0)$) obtained from the macroscopic rheometer experiment are included in this figure. Our first observation is that the trends in G' are well reproduced by the EW data. For the 2 and 10 wt % gelatin systems, even a quantitative agreement is found. Considering potential reasons why the micro- and macroscopic measurements could be different (to be discussed in section 4), the agreement is surprisingly good. For 5 wt % gelatin, four EW measurements with drop sizes ranging from 2 to 20 μL − the smallest one being obtained with interdigitated electrodes − produced a consistent behavior, which, however, deviates from the macrorheological experiment. (Tentatively, we attribute this slight discrepancy to an unintended deviation in the cooling protocol of this specific macrorheology measurement, for which the cooling rate was 2.5 °C/hr instead of 4 °C/hr for the EW experiments. As a consequence, the sample had more time to develop its gel network during the measurement and thus appears harder.)

From the (estimated) error bars in the EW data, it becomes clear that the typical range of elastic moduli that can be addressed is ∼10−1000 Pa. Here, the lower bound is due to the dominance of the contribution by the interfacial tension, whereas the upper bound is caused by the inaccuracy of measuring EW curves with small slopes.

4. Discussion

4.1. Comparison of *G* Values Obtained with Micro (EW) and Macro (Rheometry) Methods. We find the results obtained from the EW experiments and analysis encouraging: the droplet shapes show significant and measurable changes as they become more elastic. The range of elasticities that are measurable via the EW response extends about 1 to 2 orders of magnitude above and below the value $GR_0/\gamma = 1$. This establishes the EW method at least as a semiquantitative tool for measuring elastic properties of soft matter. The question of whether, in general, measurements of G using electrowetting should even be regarded as quantitative can be partly addressed. The theoretical model used to extract the elastic modulus showed fairly good linearity, but it was also noted that choosing a fit range corresponding to smaller deformations could give up to 15−20% higher values for G. Another aspect is that gelatin gels are not the ideal system for rheological calibrations. They are known for their aging:[21,26,27]

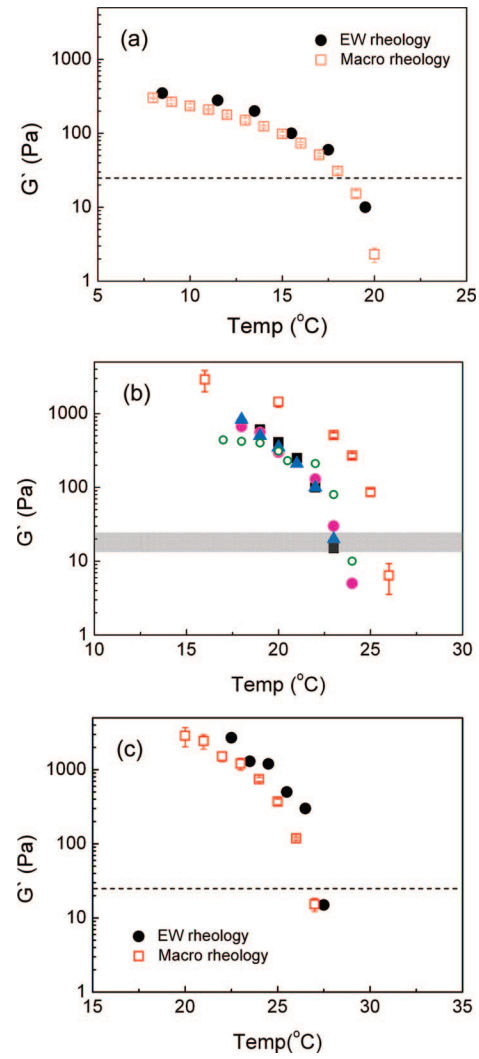

Figure 9. Comparison of microscopic and macroscopic measurements of the elastic modulus for 2, 5, and 10 wt % gelatin solutions as a function of temperature shown in (a), (b), and (c), respectively. For the 5% gelatin, droplet volumes of 10, 15, and 20 μL (solid symbols) were found to give virtually identical results. Also, on changing the geometry to a 2 μL droplet on interdigitated electrodes (open circles), the obtained G remained essentially the same. Dashed lines (a, c) and the gray bar (b) indicate the boundary $GR_0/\gamma = 1$ between elasticity and surface tension dominated behavior.

an equilibrium state (and hence elastic modulus) is never reached, and the path toward this hypothetical state depends on the thermal history. Finally, the strain fields may not be identical in EW and macrorheology. The measuring geometry used in our rheometer was designed for applying a constant shear deformation, but in the wire/droplet/plate geometry of the EW experiment, the strain fields are less uniform.

To further investigate these aspects, it would be commendable to extend the range of aqueous fluids to other elastic complex fluids, which are less sensitive to aging, like polyacrylamide gels, or PEO/PEG mixtures as described in ref 28. Numerical simulations could be performed to obtain the 3D strain field in elastic droplets deformed via EW; and finally, also new types of experiments could be considered: for example, embedding colloidal probe particles inside the gelatin droplets could allow an independent measurement of the linear viscoelastic properties

(26) Uricanu, V. I.; Duits, M. H. G.; Nelissen, R. M. F.; Bennink, M. L.; Mellema, J. *Langmuir* **2003**, *19*(20), 8182–8194.

(27) Uricanu, V. I.; Duits, M. H. G.; Filip, D.; Nelissen, R. M. F.; Agterof, W. G. M. *J. Colloid Interface Sci.* **2006**, *298*(2), 920–934.

via particle tracking microrheology.[29] Using larger particles or stiffer gels, in principle also the 3D strain field caused by EW could be measured, for example using confocal fluorescence microscopy.

4.2. Range of Measurable Elasticities. The working range of elastic moduli that can be addressed with the EW method was found to be ~10−1000 Pa for the gelatin droplets studied. Because the lower limit is set by the interfacial tension, adding surfactant (as we tested), or using a different oil to lower γ, could be used to extend the lower side of the working range. Because the elastic effects scale as GR/γ, also larger droplets could be used to make the elastic contribution more prominent. As a rule of thumb, surface tensions can be reduced by a factor 3. The droplet radius can be changed between ~0.3 mm, related to the thickness of the platinum wire, and ~3 mm, related to the Bond number. The latter, $B_o = R^2 g \Delta\rho/\gamma$ should be $\ll 1$ to keep the influence of gravity on droplet shape negligible. In the present study, $\Delta\rho$, the difference in density between the ambient and the drop phase was varied between 0.04 g/mL (silicone oil) and 0.25 g/mL (dodecane). For a droplet with radius 3 mm, $B_o \approx 0.05$ requires $\Delta\rho \approx 0.01$ g/mL. This estimated practical limit could be achieved with perfluorinated silicone oils. Summarizing, the accessible range for G might be stretched to ≈ 3−3000 Pa. This makes the EW method very suitable to study soft matter.

5. Outlook

5.1. Microfluidic Applications. The good repeatability of the EW experiment, evidenced by Figure 5, indicates interesting perspectives for applications of jellifying droplets in EW-based digital microfluidics (EWDM) applications, in which large numbers of drops have to be actuated reliably, using the same set of electrodes. At least for gelatinized droplets, possibilities for actuation (i.e., letting droplets make discrete steps from one electrode to another) seem within reach. Interestingly, gelatin capsules are also known as carriers in drug delivery (DD) (e.g., ref 30). Potentially the combination of DD and EWDM could thus be used to develop, test, and optimize DD strategies.

Another potential application, in which not only droplet actuation but also rheological characterization is done with EW, is that of aqueous phases that can form gels in situ. For example, one could follow polymerization reactions induced on-chip by temperature change, by light,[31,32] or by mixing with (the contents of) another droplet, or induced off-chip. To illustrate this principle, we applied a temperature quench to a gelatin droplet and followed its gelation by continually measuring $\theta(U)$ curves (this experiment was still performed with a wire/substrate geometry). Then, using the model of section 3.3 to analyze the data, the elastic modulus can be calculated as a function of time. Figure 10 shows the result of this exploratory experiment. Up to 12 min after the quench, no changes are observed, but then suddenly the gel forms and develops over (aging) time. Thus, both the incubation time and aging can be studied. Experiments and analysis like this can be automated, making it possible to obtain real-time measurements of G. A time resolution of 10 s has already been reached for the wire-substrate geometry, but could be further improved. Having the setup realized on chip, also the (relatively tedious) optical analysis of droplet deformation could be replaced by electric detection. Because the electric capacitance of a droplet in EW is proportional to its contact area, current measurements at the electrodes, as in ref 33, could provide a sensitive, quick, and reliable way of detecting mechanical changes in the droplet interior.

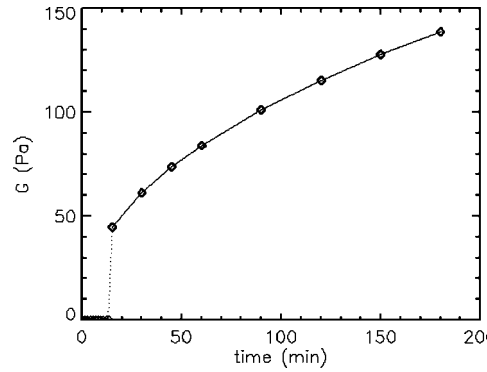

Figure 10. Online measurement of gel formation inside a small droplet. A droplet with 5 wt % gelatin was cooled from 40 to 23 °C within a few minutes and subsequently monitored over time while taking voltage ramps. Using the contact angles fitted to the droplet images, and applying our theoretical model, the elastic modulus was calculated.

5.2. Extensions of the Method to Other Rheological Quantities. Whereas the present article was focused at measuring the static elastic modulus, the rheological applications of EW are not principally restricted to this quantity. Also, viscosity or viscoelasticity (the latter being a signature of many complex fluids), should be addressable through actuation with EW. One possibility would be to study the time-dependent response of a viscoelastic droplet after a step (up or down) in voltage. Alternatively, viscoelasticity could also be studied in the frequency domain by applying sinusoidal voltage ramps. In either case, the dynamic range for measuring rheological properties will eventually be limited by the characteristic time(s) of the droplet. For viscous drops, the hydrodynamic response times are determined by a balance between the surface tension, viscosity, and density of the droplet phase, where the relative importance of each is given by the Ohnsesorge number.[34] Under usual EW conditions, these times are much longer than the time it takes the droplet to change its contact angle.

For certain droplet systems, one could measure the rheological properties of the interface instead of those of the bulk. This could apply for example to capsules or other particles having a liquidlike interior and an elastic or viscoelastic coat.

Another unexplored possibility is the measurement of nonlinear rheological properties like the yield stress. Because materials exhibiting this behavior are elastic up to the yield point, this measurement could turn out to be a straightforward extension of the already applied method, to larger (Maxwell) stresses. The signature of yielding (and recovery) should then be measurable via the magnitude of the apparent elastic modulus G. Especially for very fragile (i.e., low critical strain) materials like certain associating polymers (e.g., ref 35), fibrous networks of molecular gelators[36] or colloids aggregated via short ranged forces (e.g., ref 37) with highly controlled and as gentle loading as possible with EW could enable these delicate measurements.

6. Conclusions

Electrowetting experiments using a 3D (sessile drop + wire) geometry have convincingly shown that the deformation of gelled

(28) Dontula, P.; Macosko, C. W.; Scriven, L. E. *AIChE J.* **1998**, *44*(6), 1247–1255.
(29) Breedveld, V.; Pine, D. J. *J. Mater. Sci.* **2003**, *38*(22), 4461–4470.
(30) Vandelli, M. A.; Rivasi, F.; Guerra, P.; Forni, F.; Arletti, R. *Int. J. Pharm.* **2001**, *215*(1−2), 175–184.
(31) Dendukuri, D.; Pregibon, D. C.; Collins, J.; Hatton, T. A.; Doyle, P. S. *Nat. Mater.* **2006**, *5*(5), 365–369.
(32) Nie, Z. H.; Xu, S. Q.; Seo, M.; Lewis, P. C.; Kumacheva, E. *J. Am. Chem. Soc.* **2005**, *127*(22), 8058–8063.
(33) Verheijen, H.J. J.; Prins, M. W. J. *Rev. Sci. Instrum.* **1999**, *70*(9), 3668–3673.
(34) Baret, J.-C.; Decré, M. M. J.; Mugele, F. *Langmuir* **2007**, *23*(9), 5173.

aqueous droplets is not only determined by the surface tension but also by the elastic properties of the fluid. The working range for moduli, which give a measurable elastic contribution to the EW response, was found to lie between 10 and 1000 Pa, but could be extended by half a decade in both directions. This makes the method suitable for soft materials. A model based on Hertz theory was used to extract the elastic shear modulus from the measured electrowetting curves. Comparing the elastic moduli extracted from EW with macroscopic rheology data, a quantitative agreement could be obtained in the indicated working range. This creates interesting perspectives for using EW on chip, not only as a tool to actuate complex aqueous fluids but also to measure their surface tension and rheology.

Acknowledgment. We thank Eko Purnomo for assisting with the rheometer experiments. A.G.B. acknowledges the BOYSCAST fellowship from the Indian government.

Note Added after ASAP Publication. This article was published ASAP on December 11, 2008. A change has been made in the title. The correct version was published on December 16, 2008.

LA803080K

(35) Wientjes, R. H. W.; Duits, M. H. G.; Jongschaap, R. J. J.; Mellema, J. *Macromolecules* **2000**, *33*, 9594–9605.
(36) de Loos, M.; Friggeri, A.; van Esch, J.; Kellogg, R. M.; Feringa, B. L. *Org. Biomol. Chem.* **2005**, *3*, 1631–1639.
(37) Tolpekin, V. A.; Duits, M. H. G.; van den Ende, D.; Mellema, J. *Langmuir* **2004**, *20*, 2614–2627.